Iowa Research Online
The University of Iowa's Institutional Repository

University of Iowa
Iowa Research Online

Theses and Dissertations

Fall 2014

Temperature effects on the potential window of water and acetonitrile and heterogeneous electron transfer rates of outer sphere redox probes

Emily Mrugacz Null
University of Iowa

Copyright 2014 Emily Null

This thesis is available at Iowa Research Online: http://ir.uiowa.edu/etd/1491

Recommended Citation
Null, Emily Mrugacz. "Temperature effects on the potential window of water and acetonitrile and heterogeneous electron transfer rates of outer sphere redox probes." MS (Master of Science) thesis, University of Iowa, 2014.
http://ir.uiowa.edu/etd/1491.

Follow this and additional works at: http://ir.uiowa.edu/etd


Part of the Chemistry Commons

TEMPERATURE EFFECTS ON THE POTENTIAL WINDOW OF WATER AND ACETONITRILE AND HETEROGENEOUS ELECTRON TRANSFER RATES OF OUTER SPHERE REDOX PROBES

by
Emily Mrugacz Null

A thesis submitted in partial fulfillment
of the requirements for the Master of
Science degree in Chemistry
in the Graduate College of
The University of Iowa

December 2014

Thesis Supervisor: Associate Professor Johna Leddy

Copyright by

EMILY MRUGACZ NULL

2014

All Rights Reserved

Graduate College
The University of Iowa
Iowa City, Iowa

CERTIFICATE OF APPROVAL

MASTER'S THESIS

This is to certify that the Master's thesis of

Emily Mrugacz Null

has been approved by the Examining Committee for the thesis requirement for the Master of Science degree in Chemistry at the December 2014 graduation.

Thesis Committee:

Johna Leddy, Thesis Supervisor

Edward Gillan

Scott Shaw

To My Family

ACKNOWLEDGMENTS

First, I would like to thank Dr. Leddy for her wisdom, guidance, and support. I would also like to thank group members, past and present: Krysti Knoche, Jeff Landgren, Garett Lee, Matt Lovander, Jacob Lyon, Perry Motsegood, Tim Paschkewitz, and Nadeesha Rathuwadu for sharing their knowledge, friendship, and sometimes needed coffee breaks.

To my wonderful husband, Jordan, I don't know how to say thank you enough. Thank you for keeping me sane and for your encouragement every day. I would also like to thank my parents, Gary and Rebecca Mrugacz, and my sister, Jeanne Mrugacz, for their continual love and support.

Finally, I am grateful to the National Science Foundation and the University of Iowa Department of Chemistry.

ABSTRACT

This thesis examines the effects of temperature on the electrochemistry of an aqueous solvent, HNO_3, and a non aqueous solvent, acetonitrile and their respective analytes. It has been demonstrated previously that lowering the temperature of a solvent expands the available potential window in which to perform electrochemical experiments. The working window of an aqueous solvent is limited by the electrolysis of water. Cyclic voltammetry was utilized to examine the temperature effects on the rates of the oxidation and reduction of the solvent as well as the effects on the redox species in solution.

The redox species experienced decreased peak splitting with lower temperatures, and the diffusion constants and rate constants were lowered as the temperature decreased. It was determined that the solvent window of the HNO_3 solution was extended in experiments conducted at lower temperatures. The voltage window went from 2.349 V at 25 °C to 2.671 V at 5 °C using a glassy carbon working electrode. No significant improvement in the voltage window of acetonitrile was seen at lower temperatures. Rate constants for the oxidation and reduction of water were lowered and the voltage window of nitric acid expanded.

PUBLIC ABSTRACT

Electrochemical reactions are processes where the transfer of electrons is involved. Electrochemical reactions are part of many everyday items including batteries and fuel cells. Cyclic voltammetry is one technique that is used to analyze these systems. Cyclic voltammetry is carried out by applying a voltage to an electrode and measuring the current that is produced as the potential is scanned through a range of voltages. To carry out cyclic voltammetry, a solvent and electrolyte are needed. The span of the voltages able to be used is typically limited by the solvent in aqueous cases, where water is electrolyzed.

In this study, the effect of temperature on the solvent during cyclic voltammetry is examined. It is found that lowering the temperature of an aqueous solution extends the solvent window, and thus the range of potentials that can be utilized. This may be useful for analyzing compounds that are typically out of the available solvent window.

TABLE OF CONTENTS

LIST OF TABLES

Table

LIST OF FIGURES

Figure

CHAPTER 1

INTRODUCTION

1.1 Background

Electrochemical techniques are limited by the solvent window. Within the solvent window, the solvent does not undergo reduction or oxidation processes, and no faradaic current is produced by solvent or electrolyte electrolysis. In aqueous solutions, the oxidation and reduction of water limit the available range of potentials over which analytes may be examined. The water oxidation reaction in acid is shown in Equation 1:

$$O_2 + 4H^+ + 4e \rightleftharpoons 2H_2O \tag{1}$$

Thermodynamically, water oxidation takes place at 1.229 V at a Pt electrode versus a normal hydrogen electrode (NHE) [1]. The water reduction reaction in base is shown in Equation 2:

$$2H_2O + 2e \rightleftharpoons H_2 + 2OH^- \tag{2}$$

The standard reduction potential of water is -0.828 versus NHE.

Nonaqueous solvents have larger voltage windows than aqueous solvents as the potential window is mainly limited by the decomposition of the supporting electrolyte salt and not the electrolysis of the solvent itself [2] For acetonitrile with tetrabutylammonium tetrafluoroborate, the potential window extends from -1.8 V to +2.8 V at a platinum electrode versus. a standard calomel electrode (SCE). [3] For both types of solvents, it would be advantageous to extend the potential window,

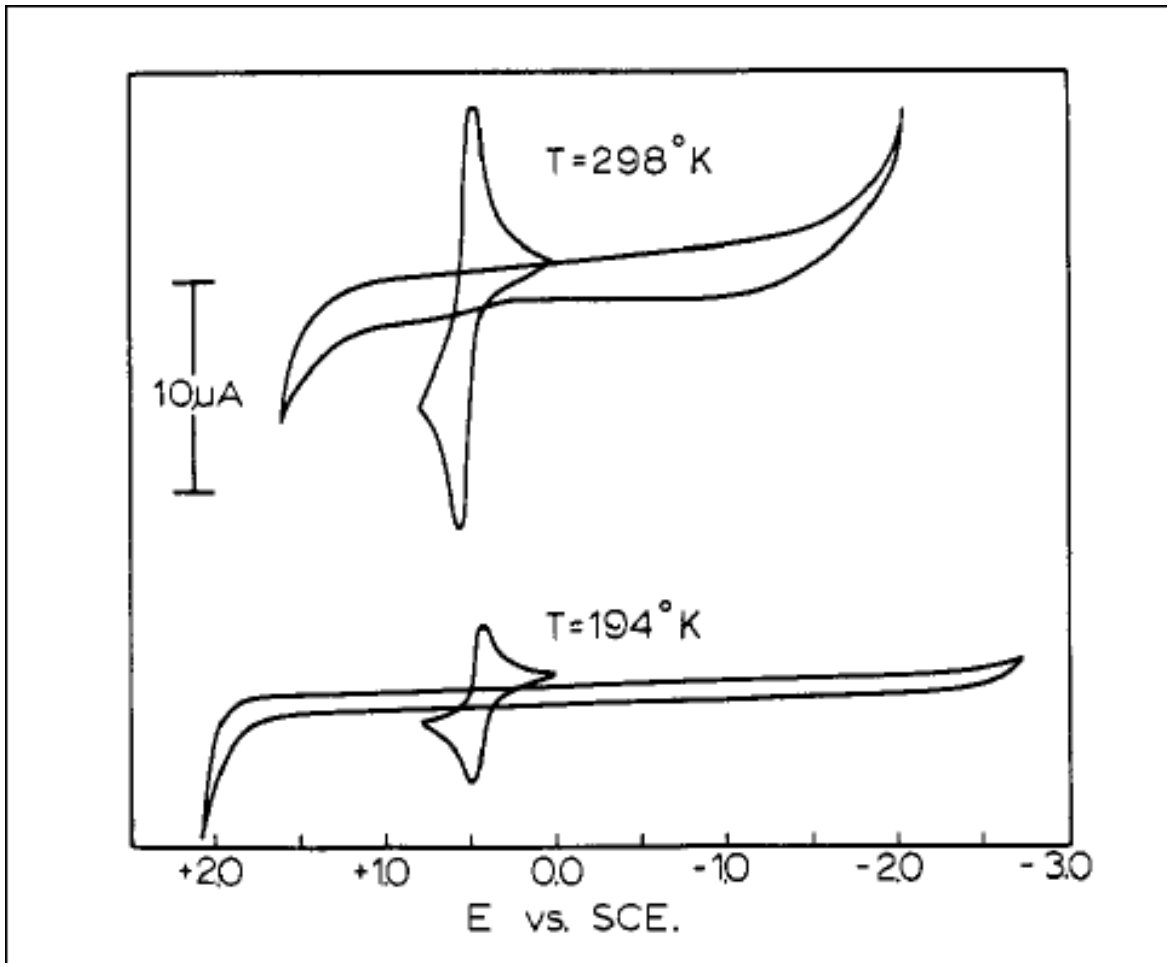

Figure 1. Effect of low temperature on the solvent window of DMFcontaining 0.1 M TBAP with scan rate of 135 mV/s. [4]

which could allow for analytes with redox potentials outside of the given potential ranges to be examined.

Temperature is one way the solvent window and the electrochemical processes can be controlled. The effect of low temperature on the solvent window of dimethylformamide (DMF) was previously studied by Van Duyne and Reilley [4]. At -79.15 °C, there was a significant expansion of the solvent window and decrease in capacitance, as shown in Figure 1.

In addition to broadening the solvent potential window, peak splittings and diffusion coefficients were also examined and modeled. It was found that for a reversible heterogeneous electron transfer process, as the temperature decreased, the peak splitting also decreased as anticipated by theory [1, 4]. This is shown in Figure 2A.

1.2 Cyclic Voltammetry

Cyclic voltammetry (CV) is an electrochemical technique where current is measured as voltage is swept over a certain potential range. It is a technique that can provide information about the kinetics of electron transfer processes, the reversibility of a reaction, and information on the thermodynamics of the system. It is therefore a useful technique for studying the effects of temperature on electrolyte solution electrolysis and electrochemical analytes (redox probes).

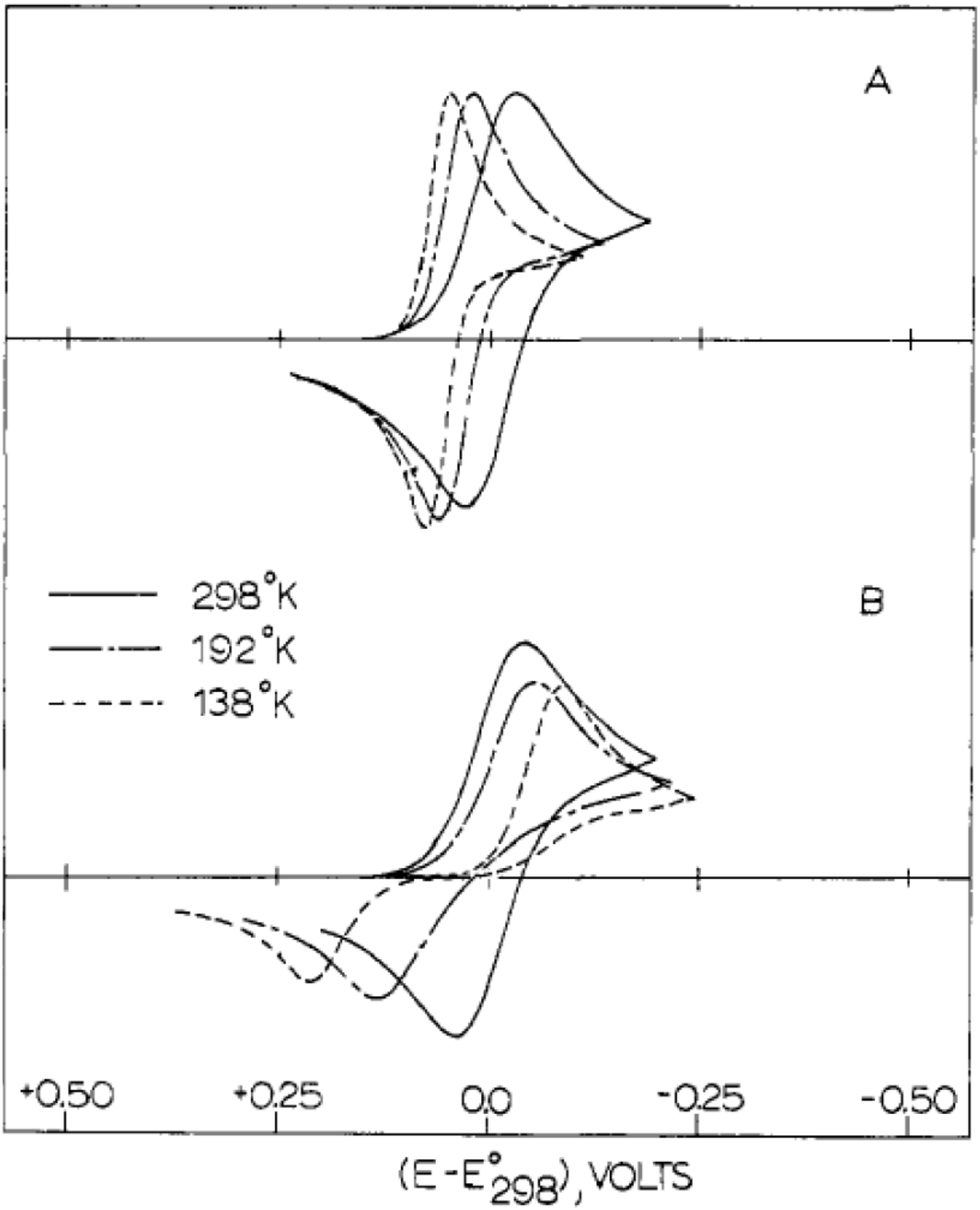

Figure 2. Impacts of temperature on rates of interfacial electron transfer are shown. A: Temperature effects on a reversible heterogeneous electron transfer. B: Temperature effects on a quasireversible electron transfer. [4]

CHAPTER 2

EXPERIMENTAL

Here, the experimental protocols are described.

2.1 Electrodes and Instrumentation

The electrochemical cell is a three electrode cell. All measurements were done by cyclic voltammetry.

2.2 Working Electrode

The working electrode was a CH Instruments, Inc., glassy carbon electrode (GCE) with a geometric area of 0.071 cm^2. To ensure surface reproducibility of the electrode, a standard cleaning procedure was followed before each use. The electrode was manually polished on a polishing cloth with 1.0, 0.3, and 0.05 μm alumina powder (Buehler) slurries, successively. The electrode was rinsed with deionized water between each grit and prior to each use.

2.3 Counter and Reference Electrodes

The counter electrode was a high surface area platinum mesh. It was cleaned by soaking in concentrated nitric acid for five minutes and rinsing with deionized water. Two different reference electrodes were used. A saturated calomel electrode (SCE) was used for the aqueous solution and a silver wire quasireference electrode served for the nonaqueous measurements. The SCE was cleaned with deionized water and

dried with a Kimwipe. The silver quasireference electrode was cleaned by soaking in nitric acid for five minutes and rinsed with deionized water, and then acetonitrile.

2.4 Voltammetry

A CHI 760B potentiostat was used for all cyclic voltammetric data. The voltammograms were collected at scan rates varying from 10 to 500 mV/s. Scans were performed in sets of three, in a randomized order to identify any time dependent degradation in electrode performance.

2.5 Temperature Control

Solution temperature was controlled by a Netlab RTE 17 Refrigerated Bath (Thermo Electron Configuration) connected to a water jacketed vessel. The setup is shown in Figure. 3. Temperatures from 5 to 70 °C were examined. Solution temperature was measured with a Fluke 62 Mini IR Thermometer.

2.6 Solvents

Two different solvents were investigated for temperature effects. An aqueous solution of 0.1 M HNO_3 (Fisher) with 2.0 mM tris(bypyridine)ruthenium(II) chloride (Fisher) and a nonaqueous solution of 2.0 mM ferrocene (Fisher) with 0.1 M tetrabutylammonium tetrafluoroborate ($TBABF_4$) (Sigma Aldrich) in acetonitrile (Fisher) were used. All solutions were purged through a frit with nitrogen gas for 15 minutes before data collection and were kept under a nitrogen blanket for the duration of the experiments.

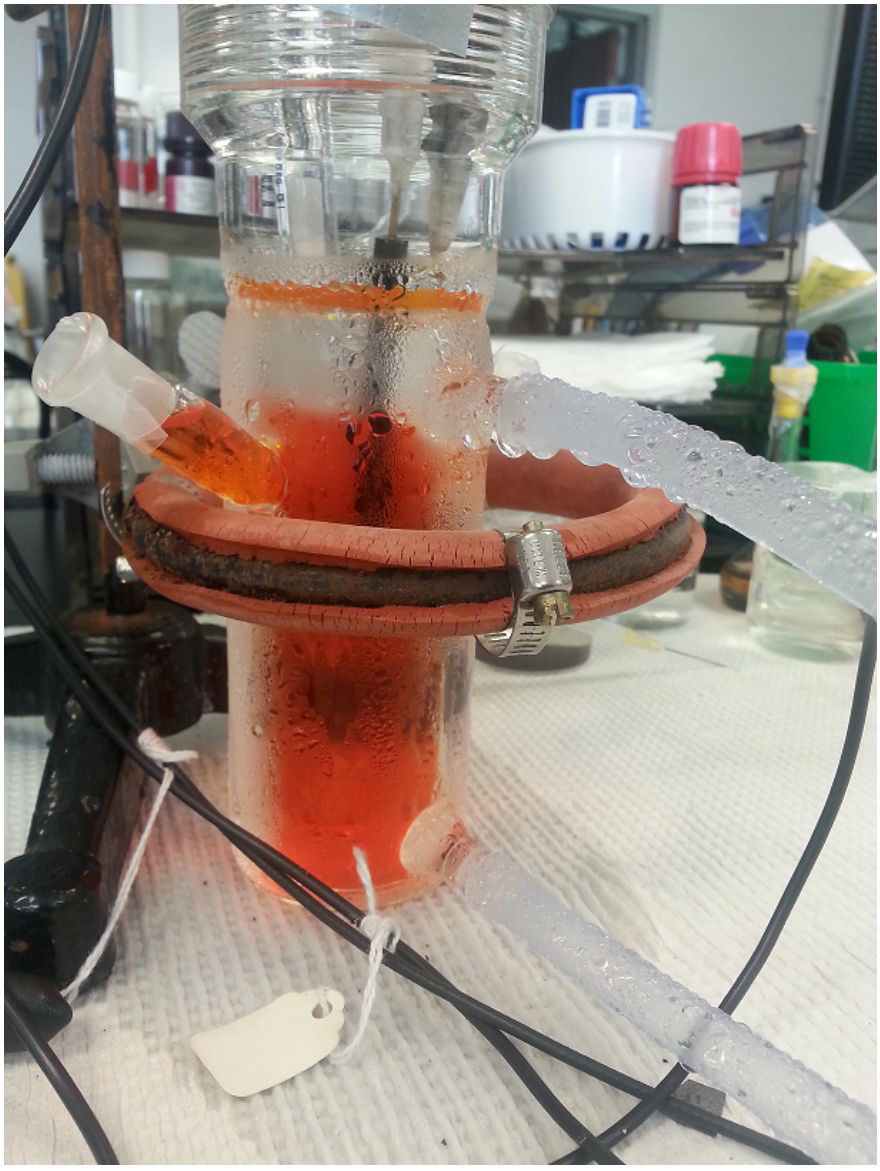

Figure 3. Experimental Setup: The $Ru(bpy)_3^{2+}$ solution is orange and contained within the jacketed cell. The temperature of the cell is controlled by flow of heated or cooled water that enters and exits the jacket volume through the Tygon tubing on the right front of the photo. The three connections to the electrodes are visible at the top of the cell.

CHAPTER 3

RESULTS AND DISCUSSION

3.1 Aqueous Solvent

The aqueous solvent is water with 0.1 M HNO_3.

3.1.1 Scan Rate Studies

Cyclic voltammetry of 2.0 mM tris(bypyridine)ruthenium(II) chloride in 0.1 M HNO_3 was done with scan rates from 10 to 500 mV/s. The electroactive cation is $Ru(bpy)_3^{2+}$.

$$Ru\,(bpy)_3^{3+} + e \rightleftharpoons Ru\,(bpy)_3^{2+} \tag{3}$$

A representative voltammetric result is shown in Figure 4. Peak current increases with increasing scan rate.

3.1.2 Diffusion Coefficient of $Ru(bpy)_3^{2+}$

$Ru(bpy)_3^{2+}$ is known to undergo reversible (rapid) heterogeneous electron transfer in aqueous electrolyte at room temperature. For a reversible electron transfer, the scan rate of cyclic voltammetry is sufficiently slow that the electron transfer at the electrode solution interface is relatively fast and A reversible and diffusion driven electron process is described by the Randles-Sevcik equation [1]:

$$i_p = 0.4463(\frac{F^3}{RT})^{\frac{1}{2}} n^{\frac{3}{2}} A D_o^{\frac{1}{2}} C_o^* v^{\frac{1}{2}} \tag{4}$$

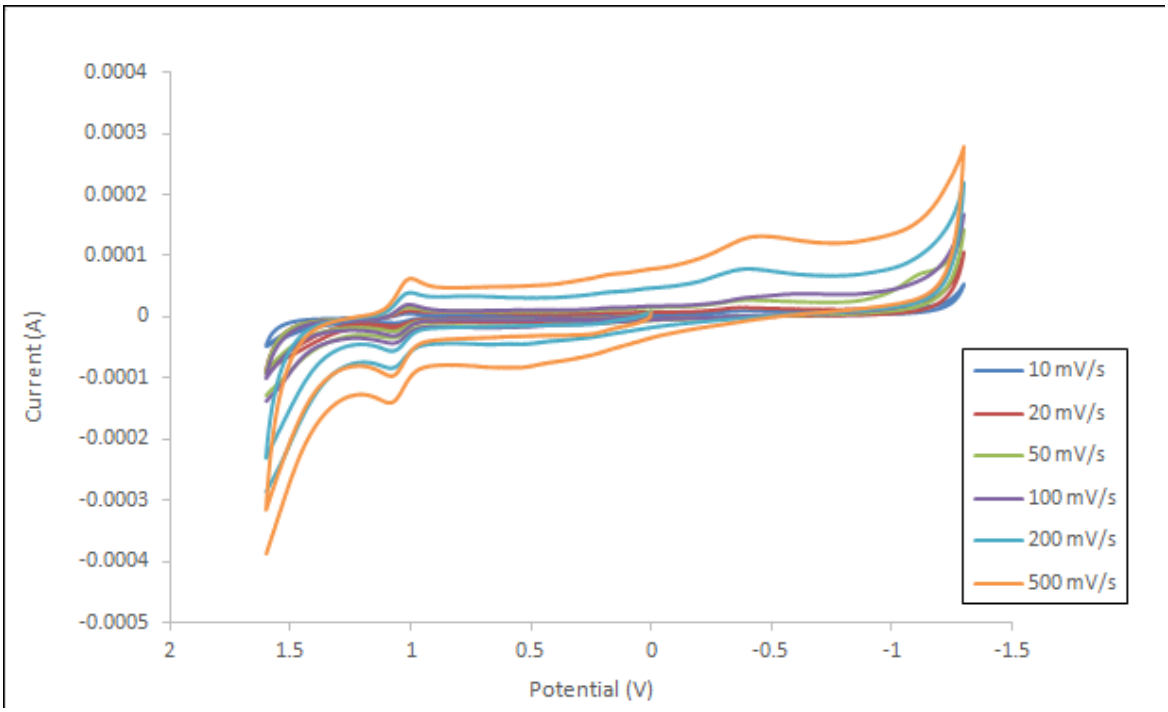

Figure 4. Overlay of $[Ru(bpy)_3]^{2+}$cyclic voltammograms at 25 °C for scan rates from 10 mV/s to 500 mV/s.

Table 1. Diffusion Coefficients of $Ru(bpy)_3^{2+}$

Temperature (°C)	Diffusion Coefficient (cm^2/s)	Regression Equation	R^2
5	$(2.6 \pm 1.0) \times 10^{-6}$	$y = (0.029 \pm 0.009)x + (59.5 \pm 2.0)$	0.734
10	$(4.1 \pm 0.9) \times 10^{-6}$	$y = (0.028 \pm 0.005)x + (58.3 \pm 1.1)$	0.883
25	$(6.9 \pm 1.1) \times 10^{-6}$	$y = (0.026 \pm 0.006)x + (61.6 \pm 1.3)$	0.820
50	$(9.2 \pm 1.9) \times 10^{-6}$	$y = (0.054 \pm 0.010)x \pm (60.1 \pm 2.3)$	0.874

where i_p is the peak current (A), n is the number of electrons, A is the area of the electrode (cm^2), F is Faraday's constant, R is the universal gas constant, T is the temperature (K), D_o is the diffusion coefficient (cm^2/s), C_o^* is the concentration in mol/cm^3 and v is the scan rate (V/s). For all temperatures, a linear relationship between peak current and the square root of the scan rate was observed, which indicates a reversible process driven by diffusion. A representative plot is shown in Figure 5.

The diffusion coefficients for $[Ru(bpy)_3]^{2+}$ were evaluated at temperatures of 5 °C to 50 °C from the slope of the plot of the anodic peak current versus the square root of the scan rate. The diffusion coefficient at 70 °C could not be calculated due to ill-defined peak currents. The calculated diffusion coefficients are shown in Table 6. As the temperature increases, the diffusion coefficient also increases. This is likely due to decreased viscosity at higher temperatures [3], and this result agrees with data from literature [5].

Diffusion is an activated process, such that the diffusion coefficient is described by an Arrhenius relationship.

$$D(T) = D_0 \exp\left[-\frac{E_A}{RT}\right] \tag{5}$$

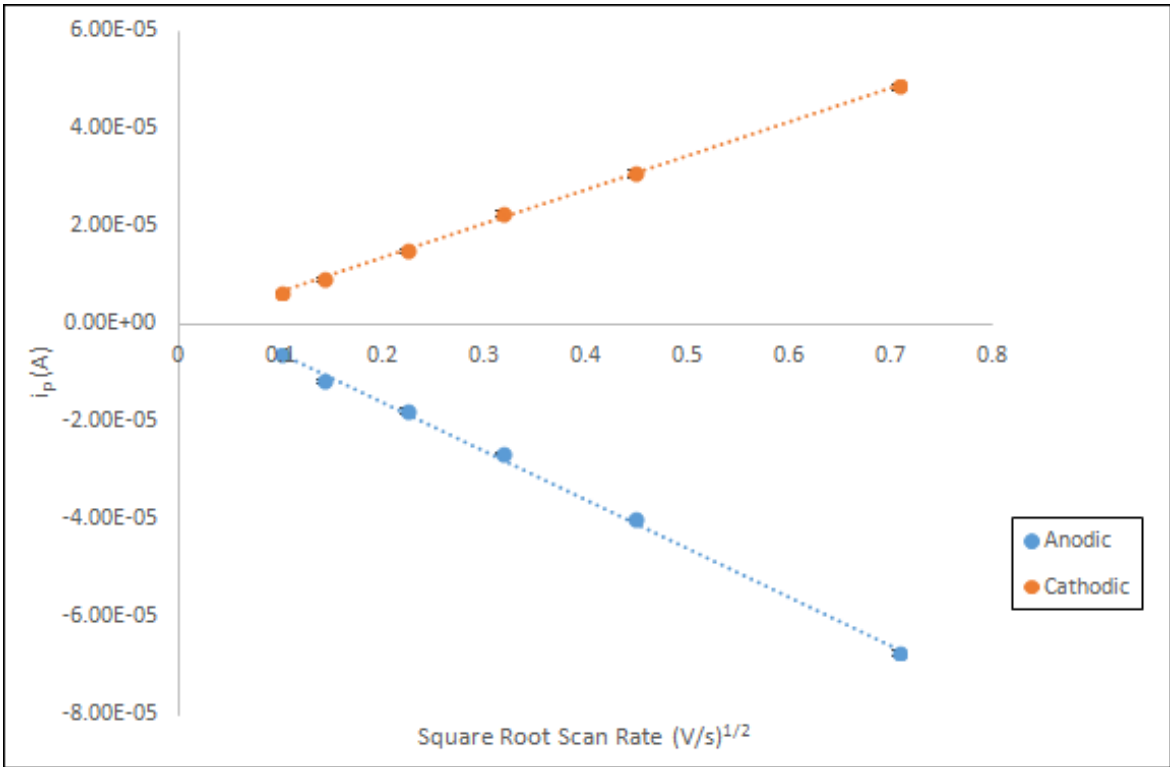

Figure 5. Peak current vs. square root of scan rate for $[Ru(bpy)_3]^{2+}$ at 25 °C. Anodic regression equation: $y = (-1.0x10^{-4} \pm 2.3x10^{-6})x + (3.9x10^{-6} \pm 8.9x10^{-7})$ with $R^2$of 0.9989. Cathodic regression equation: $y = (7.0x10^{-5} \pm 1.2x10^{-6})x + (-2.6x10^{-7} \pm 4.5x10^{-7})$ with R^2 of 0.9978.

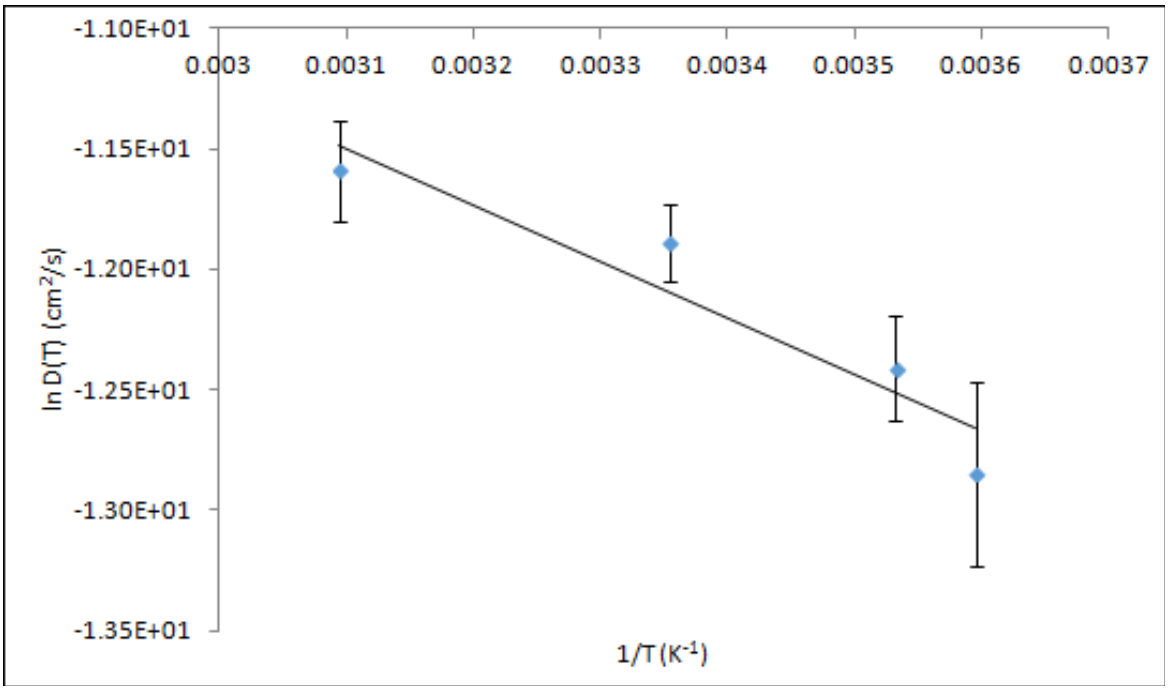

Figure 6. Arrhenius plot of lnD(T) versus 1/T for $[Ru(bpy)_3^{2+}]$ in nitric acid electrolyte

$$\ln D\left(T\right) = \ln D_0 - \frac{E_A}{RT} \tag{6}$$

A plot of $\ln D\left(T\right)$ versus $1/T$ is shown in Figure **??**. The regression line is $y = (-2.4x10^3 \pm 05.8x10^2)x + (-4.2 \pm 2.0)$ with $\mathrm{R}^2 = 0.893$. From the slope, $-E_A/R$, the activation energy for diffusion is 19.5 kJ/mol.

3.1.3 Peak Splitting

Peak splitting (ΔE_p) is defined as the absolute value of the peak voltage of the anodic process minus the peak voltage of the cathodic process, $\Delta E_p = \left|E_p^a - E_p^c\right|$. For a reversible, one electron transfer process at 25 °C,the ideal peak splitting is 57 mV. Nicholson and Shain [6] report the peak potential E_p relative to the half wave potential, $E_{1/2} = E^0 + \frac{RT}{nF} \ln \left[\frac{D_R}{D_O}\right]^{1/2}$, where E^0 is the standard potential, D_R and D_O are the diffusion coefficients for the reduced and oxidized forms of the redox probe. For most redox probes, the diffusion coefficients for the oxidized and reduced forms of the probe are within 10 %. For $D_o = D_R$, $E_{1/2}$ is E^0. From Nicholson and Shain for the reduction,

$$E_p = E_{1/2} - (1.109 \pm 0.002)\frac{RT}{nF} \tag{7}$$

Because $E_{1/2}$ is the same for both the oxidized and reduced forms, the peak splitting is

$$\Delta E_p = 2\,(1.109 \pm 0.002)\frac{RT}{nF} = (2.218 \pm 0.004)\frac{RT}{nF} \tag{8}$$

The average peak splitting values at a scan rate of 50 mV/s are shown in Figure 7. There is a general trend of increased peak splitting with increase in temperature as a

function of the scan rate, with the exception of results with a scan rate of 200 mV/s. This may be caused by the inherent imprecision in measuring the peak currents from the charging current, particularly for the reverse wave [1].

3.1.4 Solvent Window

The solvent window encompasses the range of potentials where useful faradaic measurements can be made. The onset of solvent or electrolyte electrolysis establishes the solvent potential window. Because the solvent and electrolyte are typically at concentrations many fold higher than the probe, the electrolysis current for the solvent and electrolyte will overwhelm the probe faradaic current.

The solvent window was evaluated cyclic voltammetrically. An overlay of cyclic voltammograms at different temperatures with a scan rate of 10 mV/s is shown in Figure 8.

From Figure 8, it can be seen that the voltammograms at 0 and 10 °C have an extended voltage window, while the voltammograms collected at 50 and 70 °C have a narrower working voltage window compared to the room temperature voltammogram. This trend held among all conducted scan rates. It should be noted that although the solvent limits changed, the $[Ru(bpy)_3]^{2+}$ peak potentials remained relatively unchanged, indicating this is not due to a shift in the reference electrode's potential due to the temperature.

The anodic potential limit was defined as the potential with a corresponding current of twice $[Ru(bpy)_3]^{2+}$'s anodic peak current. The cathodic potential was defined as the potential at which the current was twice the value of $[Ru(bpy)_3]^{2+}$'s

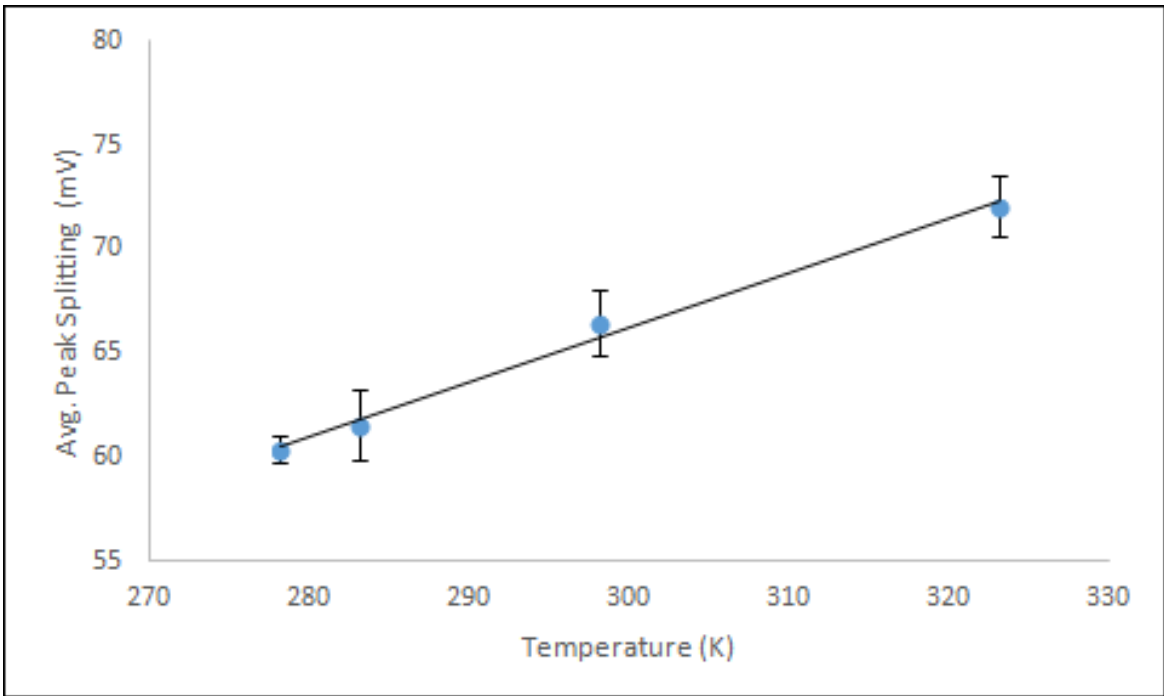

Figure 7. Average peak splitting (mV) vs. temperature at 50 mV/s. The linear regresion equation is $y = (0.26 \pm 0.02)x + (59.2 \pm 0.5)$ with an R^2 value of 0.992.

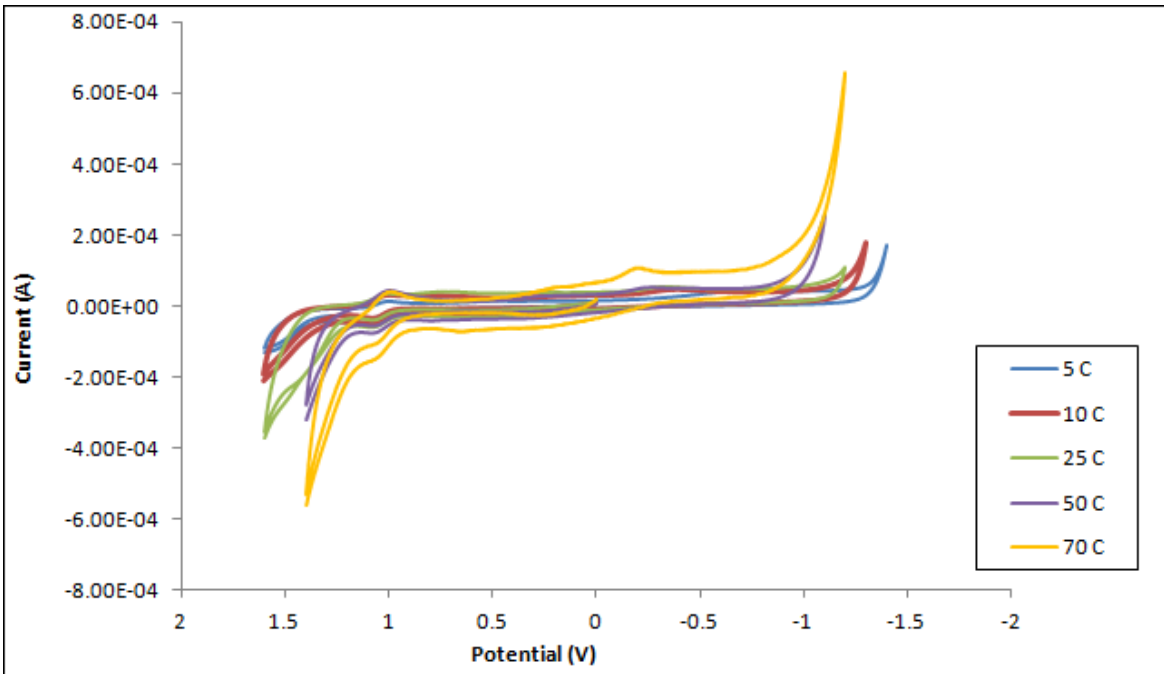

Figure 8. Overlay of $[Ru(bpy)_3]^{2+}$ cylic voltammograms at varying temperatures with a scan rate of 100 mV/s.

cathodic peak current. The average potential limits at the varying temperatures and scan rates are shown in Table 2.

Figures 9 and 10 give examples of the effect of temperature on the solvent window. The anodic limit and the cathodic limit were both extended with decreased temperature. The change in the cathodic potential limit was more apparent.

3.1.5 Rate Constants

Heterogeneous electron transfer rates were evaluated as functions of temperature and scan rate for the two probes.

3.1.5.1 Rate Constants for $Ru(bpy)_3^{2+}$

Standard heterogeneous electron transfer rate constants, k^0, are determine from the peak splitting ΔE_p as a function of scan rate v with the method of Nicholson [1, 7]. The rate of the electron transfer at the electrode solution interface is potential dependent and defined for the reduction and oxidation as

$$k_{red}(E) = k^0 \exp\left[\frac{-\alpha F}{RT}\left(E - E^{0'}\right)\right] \quad (9)$$

$$k_{ox}(E) = k^0 \exp\left[\frac{(1-\alpha) F}{RT}\left(E - E^{0'}\right)\right] \quad (10)$$

where α is the transfer coefficient. A measure of the symmetry of the electron transfer barrier, $0 \leq \alpha \leq 1$ where typically α is about 0.5. When $E = E^{0'}$, $k_{red}(E) = k_{ox}(E) = k^0$ (cm/s). Nicholson tabulated a parameter ψ as a function of ΔE_p.

$$\psi = \left[\frac{D_O}{D_R}\right]^{\alpha/2} k^0 \left[\frac{\pi D_O n F v}{RT}\right]^{1/2} \quad (11)$$

Table 2. Potential Window for Water as a Function of Temperature and Scan Rate

Temp (°C)	v (mV/s)	Anodic Potential Limit (V versus SCE)	Cathodic Potential Limit (V versus SCE)	Potential Window (V)
70	500	1.292±0.007	-0.886±0.008	2.178±0.011
	200	1.279±0.006	-0.937±0.029	2.216±0.030
	100	1.294±0.018	-1.023±0.013	2.317±0.022
	50	1.253±0.010	-0.935±0.025	2.188±0.026
	20	1.220±0.009	-0.858±0.042	2.078±0.043
	10	1.247±0.002	-0.858±0.172	2.105±0.172
50	500	1.327±0.048	-0.881±0.078	2.208±0.091
	200	1.287±0.012	-0.900±0.035	2.187±0.037
	100	1.327±0.010	-0.965±0.075	2.292±0.076
	50	1.291±0.007	-0.819±0.023	2.11±0.024
	20	1.259±0.009	-0.897±0.005	2.156±.010
	10	1.274±0.002	-0.854±0.011	2.128±0.011
25	500	1.336±0.009	-0.994±0.080	2.330±0.080
	200	1.302±0.009	-0.991±0.075	2.293±0.076
	100	1.406±0.034	-1.065±0.014	2.471±0.037
	50	1.289±0.016	-1.032±0.054	2.321±0.057
	20	1.256±0.006	-1.047±0.049	2.303±0.050
	10	1.284±0.016	-0.983±0.013	2.267±0.021
10	500	1.480±0.008	-1.039±0.102	2.519±0.102
	200	1.434±0.012	-1.095±0.066	2.529±0.067
	100	1.511±0.009	-0.983±0.046	2.494±0.047
	50	1.458±0.026	-0.999±0.065	2.457±0.071
	20	1.396±0.013	-1.051±0.024	2.447±0.022
	10	1.312±0.013	-0.945±0.044	2.257±0.046
5	500	1.415±0.004	-1.152±0.068	2.567±0.068
	200	1.393±0.018	-1.280±0.040	2.673±0.044
	100	1.432±0.011	-1.286±0.026	2.718±0.028
	50	1.374±0.017	-1.287±0.004	2.661±0.017
	20	1.396±0.011	-1.250±0.019	2.646±0.022
	10	1.395±0.034	-1.195±0.024	2.590±0.041

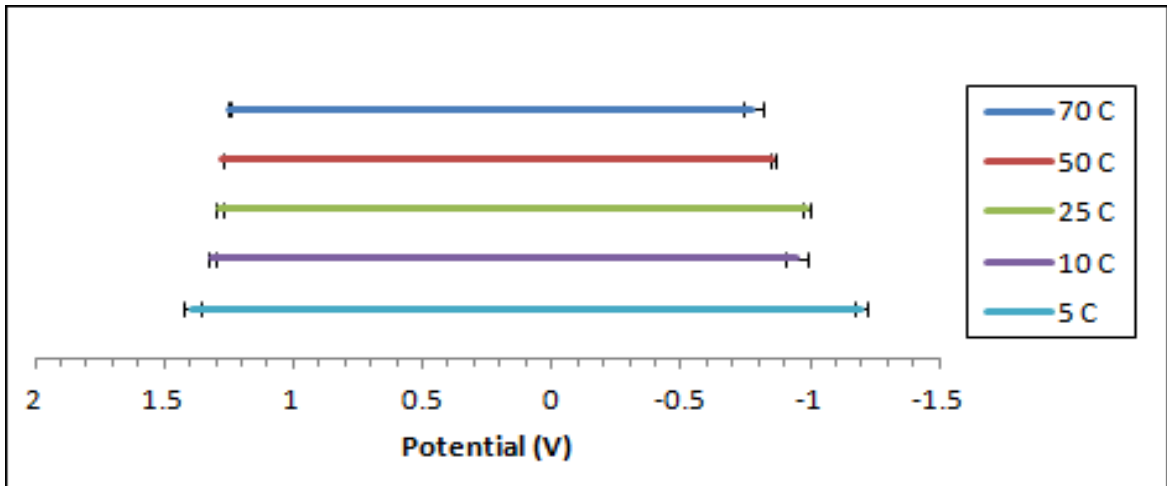

Figure 9. Effect of temperature on the solvent window with a scan rate of 10 mV/s

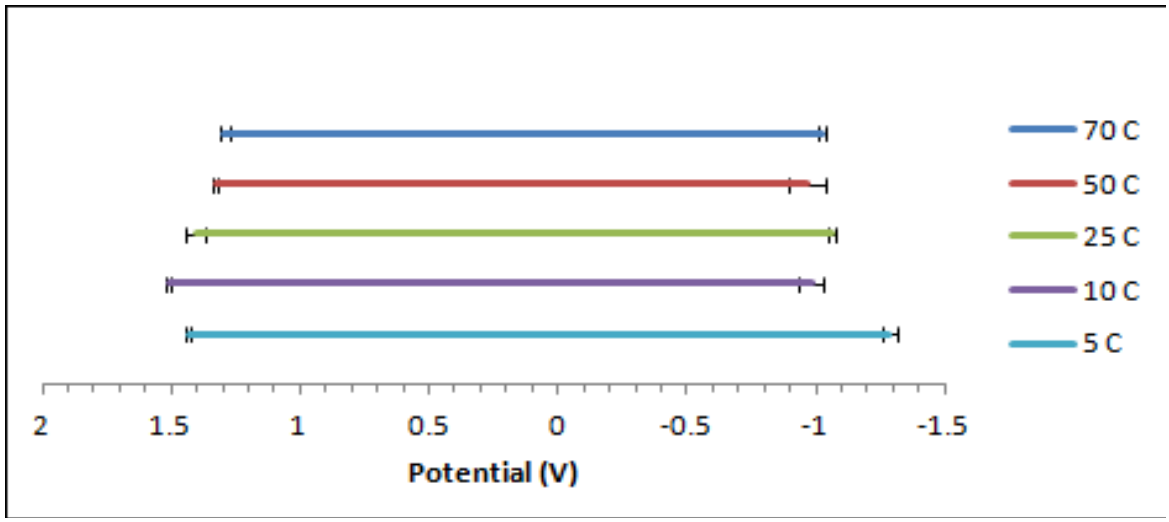

Figure 10. Effect of temperature on the solvent window with a scan rate of 100 mV/s

Subsequently, Paul and Leddy [8] showed Nicholson's result can be linearized as a plot of ΔE versus ψ^{-1} with correlation coefficients $R^2 \geq 0.996$ for α of 0.3 to 0.7. Given equation of the form $\frac{nF}{RT}\Delta E_p = M_1\psi^{-1} + B_1$, for $\alpha = 0.5$, $M_1 = (0.842_8 \pm 0.007_0)$ and $B_1 = (2.32_4 \pm 0.01_2)$ with $R^2 = 0.9960$. For an average of results for $\alpha = 0.3$, 0.4, 0.5, and 0.6, the parameters are $M_1 = (0.8416_9 \pm 0.0003_2)$ and $B_1 = (2.318_9 \pm 0.005_3)$ with $R^2 = 0.9958$, a similar outcome For $D_O = D_R$, nF/RT in volts, and substitution of M_1 and B_1 for the α-averaged values,

$$k^0 = \frac{0.8417}{\frac{nF}{RT}\Delta E_p - 2.319}\left[\frac{RT}{\pi D_O nFv}\right]^{1/2} \tag{12}$$

ΔE_p is in mV and D_O is temperature dependent and determined above, Table 1.

One criteria for reversible heterogeneous electron transfer was established by Matsuda and Ayabe [1] for linear sweep voltammetry is $\Lambda \geq 15$. From $\Lambda = k^0\left[DnFv/RT\right]^{-1/2}$, a probe sustains rapid heterogeneous electron transfer when $k^0/v^{1/2} \geq 15\left[DnF/RT\right]^{1/2}$.

The above method was applied to all the scan rates at each temperature and k^0 was determined. $k^0/v^{1/2}$ was $\gtrsim 15\left[DnF/RT\right]^{1/2}$ in all cases except the two highest scan rates (200 and 500 mV/s) at the lowest temperature, 5 °C where $k^0/v^{1/2} \geq 0.16$ is the criteria for reversibility and $k^0/v^{1/2}$ is 0.034 and 0.020 for 200 and 500 mV/s respectively. Consideration of resistance effects on the peak splitting did not increase the measured k^0 into the reversible range. It is notable that $Ru(bpy)_3^{2+}$ sustains rapid heterogeneous electron transfer rates down to temperatures of 5 °C except for the two highest scan rates.

3.1.5.2 Rate Constants for Water Oxidation and Reduction

The extended voltage window at lower temperatures can be attributed to the decreased rate constants of water oxidation and reduction at lower temperatures. To calculate the rate constant of water oxidation, a potential of 1.3 V was chosen as the location to gather current output. This voltage was far enough into the oxidation for all temperatures that it is assumed that the current is only due to the oxidation of water. The rate constants for water oxidation versus temperature collected at a scan rate of 100 mV/s are shown in Figure 12 For the water reduction rate constants, a potential of -1.0 V was selected for collecting the current. With the values of current, the rate constant was calculated by Equation 13.

$$k\left(E\right)c_{\text{solvent}} = \frac{i}{nFA} \tag{13}$$

Plots of $k\left(E\right)c_{\text{solvent}}$ are shown in Figures 11 and 12 for the reduction and oxidation respectively.

Because $k\left(E\right)$ is expected to be an activated process, Arrhenius plots of $\ln(k)$ versus $1/T$ were constructed. They are shown in Figures 13 and 14. Both the reduction and oxidation of water displayed linearity with $1/T$. The slope yields the activation energy for electrolyte electrolysis, $-E_A/R$. From this, the calculated value of the activation energy for the oxidation of water is 28.4 kJ/mol, and the value of the activation energy for the reduction of water is 7.80 kJ/mol Calculated values of the rate constants for the oxidation and reduction of water are shown in Table 3. The rate constants for the oxidation and reduction increased as the temperature increased.

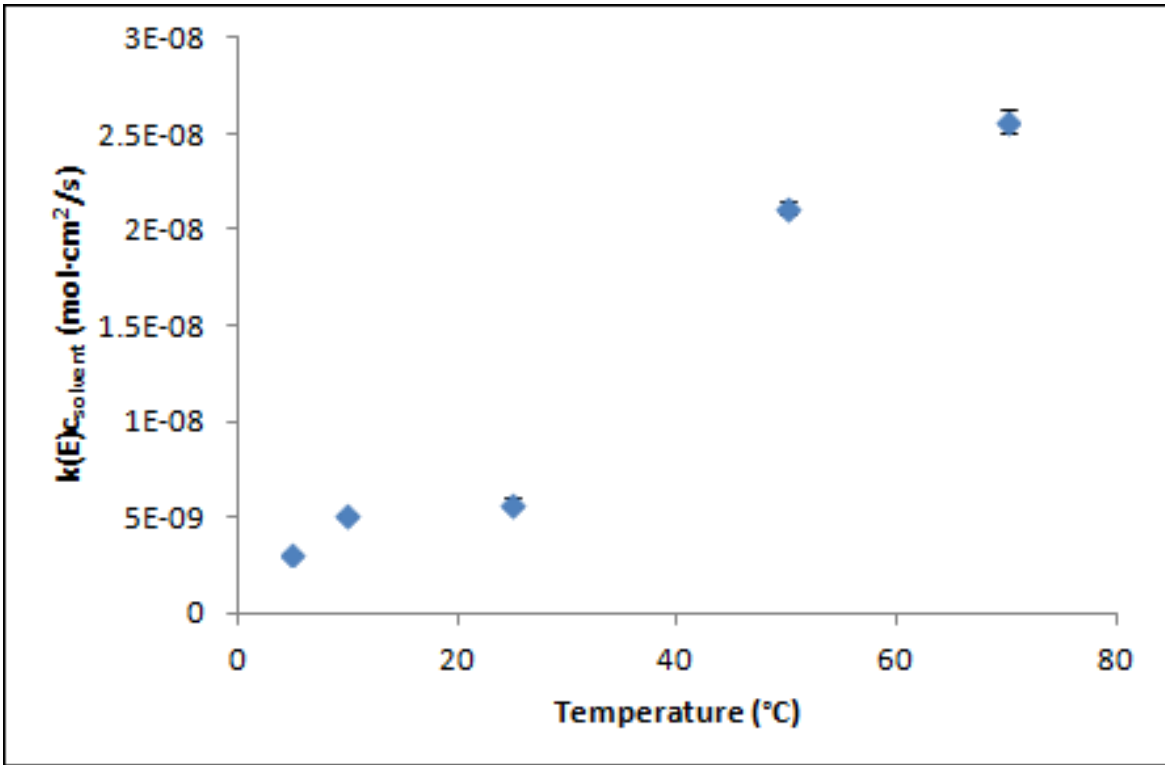

Figure 11. Rate of reduction of water as a function of temperature. Regression equation of $y = (1.22x10^{-10} \pm 1.92x10^{-11})x + (1.19x10^{-9} \pm 7.76x10^{-10})$ with $R^2 = 0.9309$.

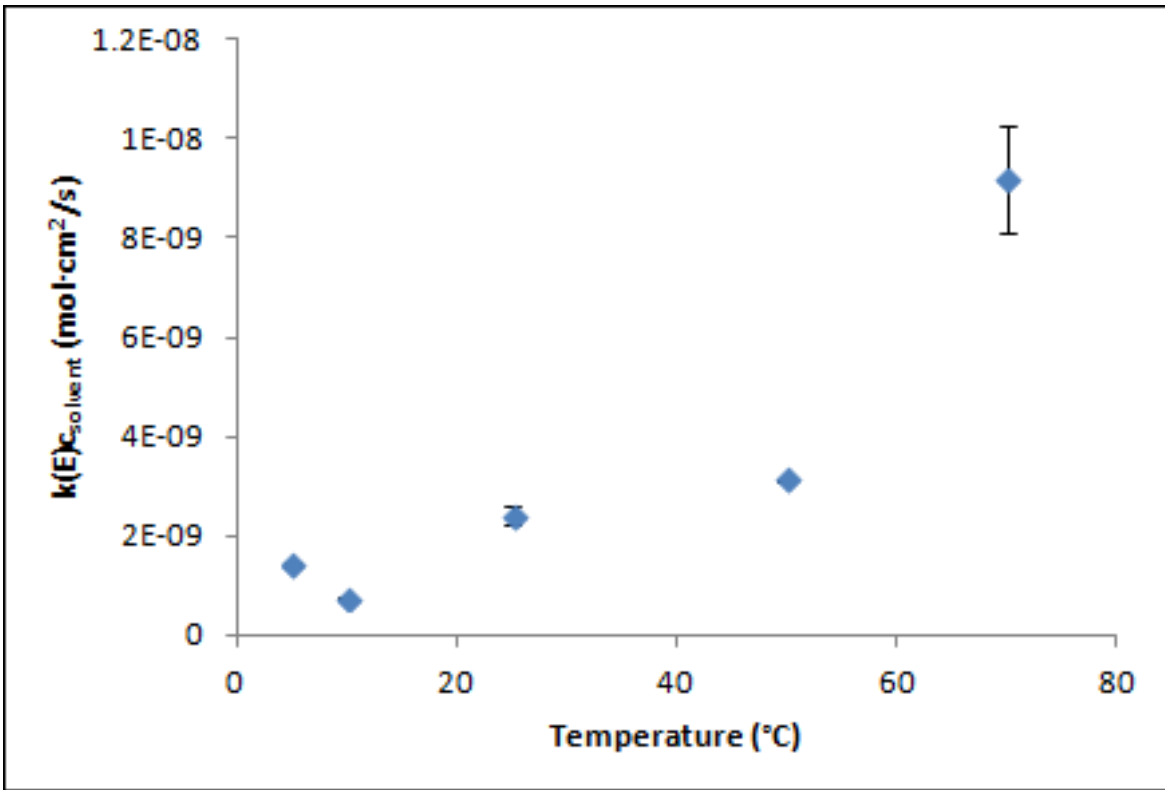

Figure 12. Rate of oxidation of water as a function of temperature. Regression equation of $y = (1.17x10^{-10} \pm 2.58x10^{-11}) + (-5.40x10^{-10} \pm 1.04x10^{-9})$ with $R^2 = 0.8721$.

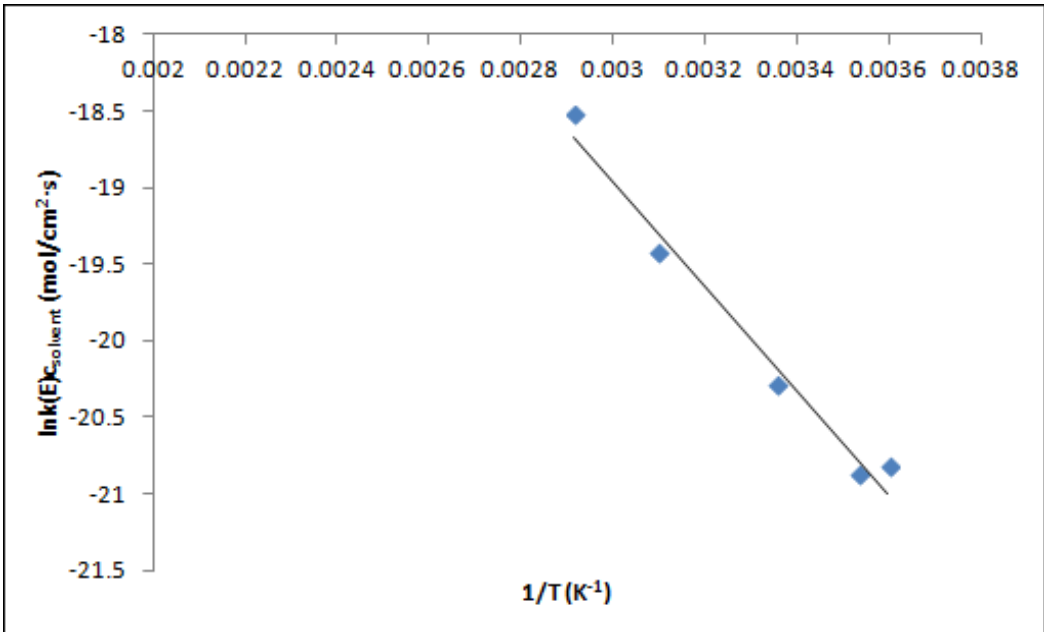

Figure 13. Arrhenius plot for the oxidation of water. Regression equation of $y = (-3.42x10^3 \pm 3.11x10^2)x + (-8.70 \pm 1.03)$ with $R^2 = 0.9759$.

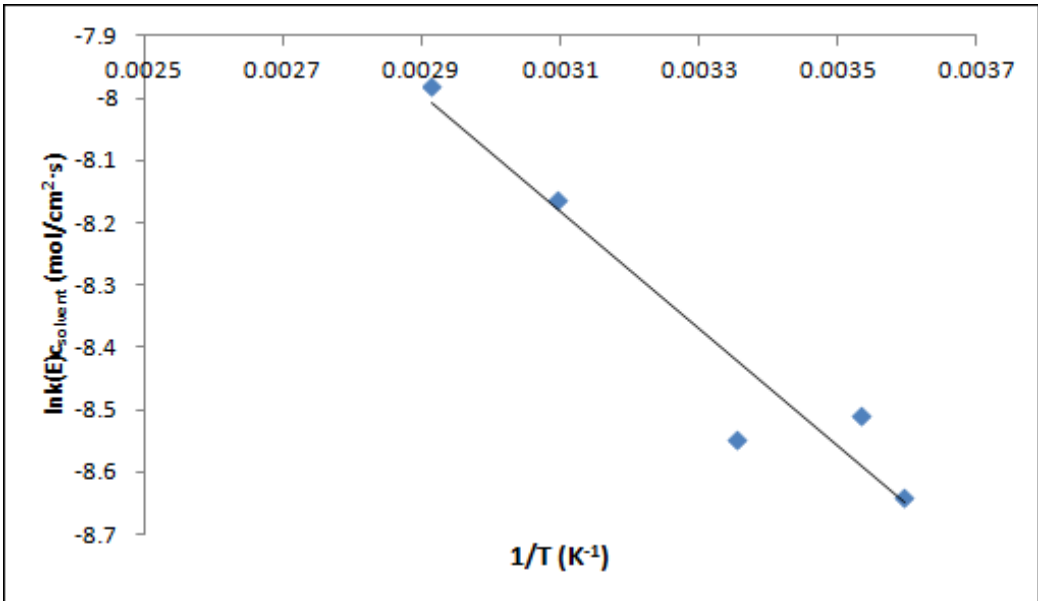

Figure 14. Arrhenius plot for the reduction of water. Regression equation of $y = (-9.38x10^2 \pm 1.52x10^2)x + (-5.27 \pm 0.50)$ with $R^2 = 0.9267$.

Table 3. Rate Parameters Determined for the Oxidation and Reduction Processes for the Water Window

Temperature (°C)	$k(E)\,c_{\text{solvent}}$ for water oxidation (cm/s)	$k(E)\,c_{\text{solvent}}$ for water reduction (cm/s)
5	9.15 x 10^{-10}	2.28 x 10^{-10}
10	8.58 x 10^{-10}	3.10 x 10^{-9}
25	1.54 x 10^{-9}	2.83 x 10^{-9}
50	3.67 x 10^{-9}	6.87 x 10^{-9}
70	9.01 x 10^{-9}	1.04 x 10^{-8}

3.2 Nonaqueous Solvent

The nonaqueous solvent is acetonitrile. Acetonitrile (H_3CCN) has a liquid range from -45 to +82 °C and a dielectric constant of 38.8.

3.2.1 Scan Rate Studies

Cyclic voltammetry of 2.0 mM ferrocene with 0.1 M $TBABF_4$ in acetonitrile was performed with scan rates from 10 to 500 mV/s. A representative result is shown in Figure 15.As expected from ferrocene, which has a reversible electron transfer, the peak currents increased with increased scan rate.

3.2.2 Diffusion Coefficient of Ferrocene

The diffusion coefficients were calculated for each temperature from the slope of the forward peak current i_p versus the square root of the scan rate, $\sqrt{v}$ All temperatures had a linear relationship between i_p and $\sqrt{v}$ and ΔE_p was invariant with v, as shown in Figure 15, consistent with a reversible (rapid) heterogeneous electron transfer rate. A representative plot is shown in Figure 16. The calculated values of ferrocene diffusion coefficient are given in Table 4. As with the diffusion

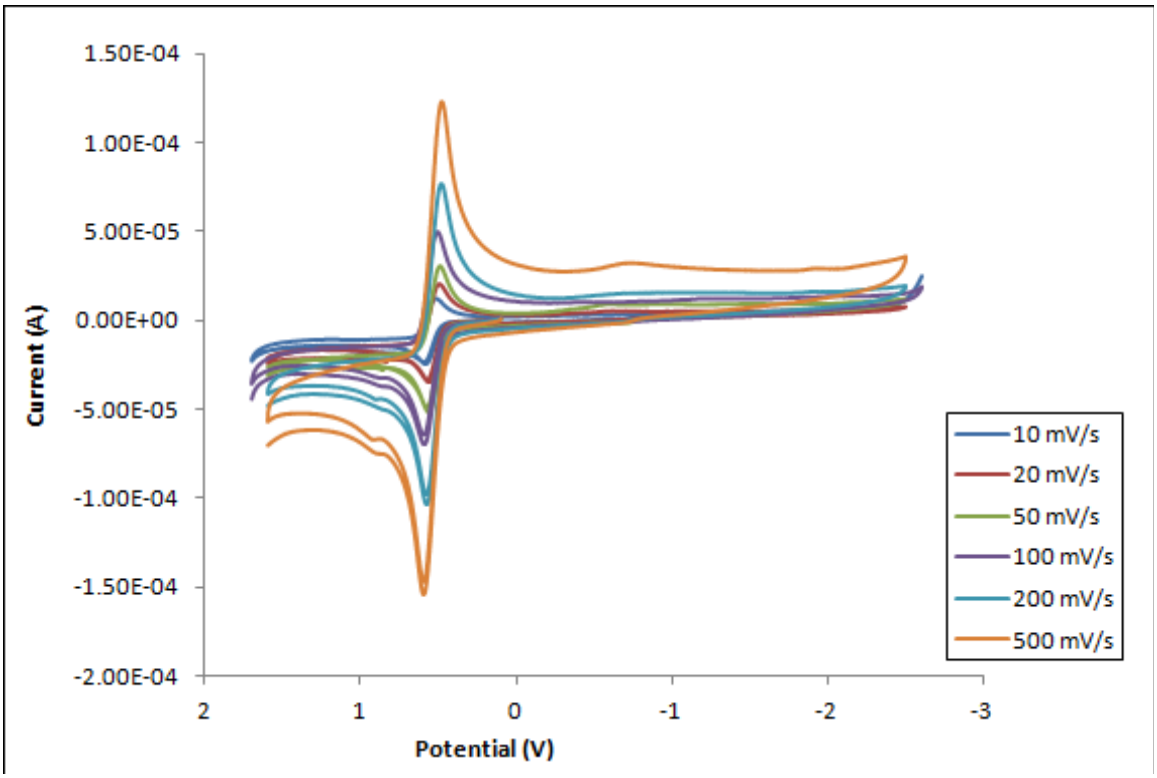

Figure 15. Overlay of cyclic voltammograms of 2.0 mM ferrocene at scan rates of 10 mV/s to 500 mV/s at 25 °C.

Table 4. Diffusion Coefficients of Ferrocene

Temp (°C)	Diffusion Coefficient (cm^2/s)	Regression Equation	R^2
5	$(2.3_9 \pm 0.2_4)$ x 10^{-5}	$y = -(1.91 \pm 0.05) \times 10^{=4}x - (5.3 \pm 2.2) \times 10^{-6}$	0.9978
10	$(2.0_5 \pm 0.4_0)$ x 10^{-5}	$y = -(1.75 \pm 0.08) \times 10^{=4}x - (6.41 \pm 0.03) \times 10^{-6}$	0.9920
25	$(2.5_4 \pm 0.2_8)$ x 10^{-5}	$y = -(1.91 \pm 0.05) \times 10^{=4}x - (3.35 \pm 0.02) \times 10^{-6}$	0.9967
50	$(3.0_1 \pm 0.3_1)$ x 10^{-5}	$y = -(2.12 \pm 0.06) \times 10^{=4}x - (5.58 \pm 0.02) \times 10^{-6}$	0.9966

Table 5. Regression Lines for Peak Splitting with Temperature for Ferrocene

Scan Rate **(mV/s)**	Regression Equation	R^2
10	$y = (0.897 \pm 0.093)x + (-185.864 \pm 27.522)$	0.9790
20	$y = (0.291 \pm 0.061)x + (-11.890 \pm 18.499)$	0.9576
50	$y = (0.120 \pm 0.016)x + (43.934 \pm 4.869)$	0.9637
100	$y = (0.202 \pm 0.033)x + (26.517 \pm 9.913)$	0.9480

coefficients of $[Ru(bpy)_3]^{2+}$in water, as temperature increased, the diffusion coefficients increased.

3.2.3 Peak Splitting

Peak splittings for ferrocene are shown in Figure 18. For scan rates 10 mV/s to 100 mV/s, peak splitting decreased linearly with decreased temperature. The regression analysis is given in Table 5.

3.2.4 Solvent Window

In contrast to the nitric acid solution, there was not an obvious extension of the solvent window for acetonitrile at lower temperatures. The results are shown in Figure 19.The oxidation potential limits are the same for 5 °C to 25 °C.The

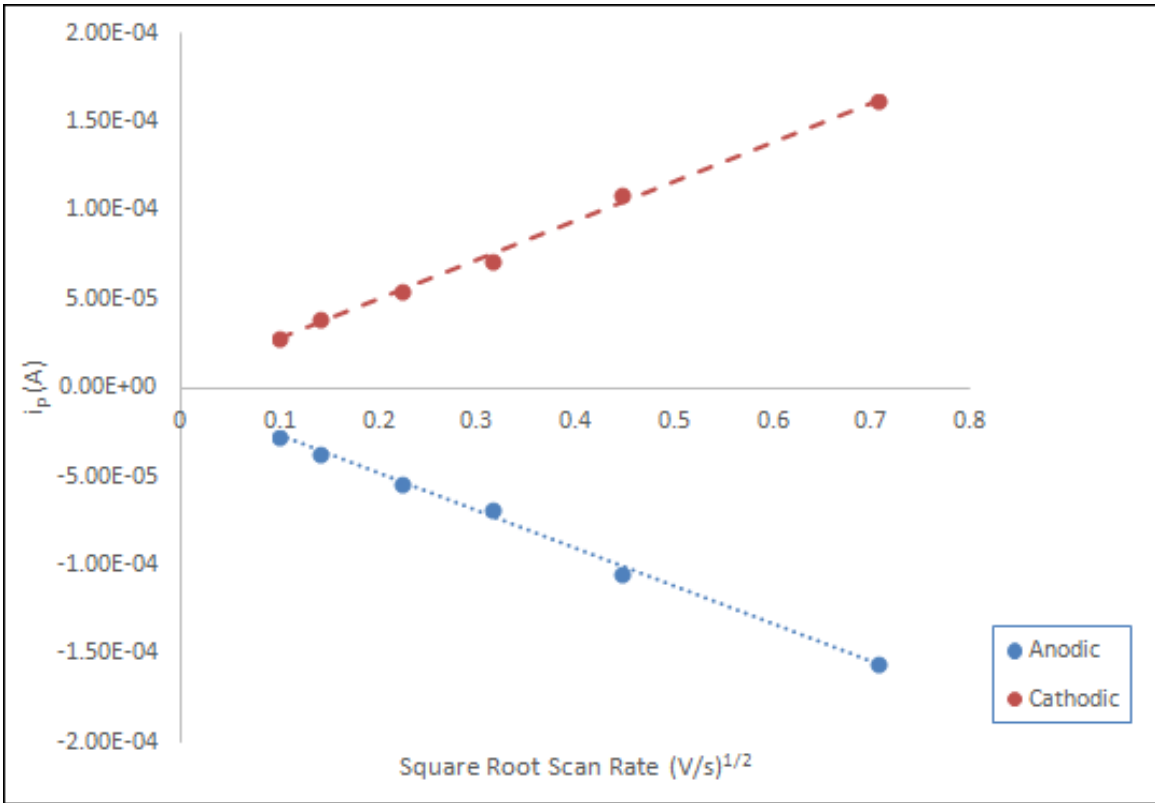

Figure 16. Peak current vs. square root of scan rate of ferrocene at 50 °C.Anodic regression equation of $y = (-2.12x10^{-4} \pm 6.17x10^{-6})x + (-5.58x10^{-6} \pm 2.36x10^{-6})$ with $R^2 = 0.9966$. Cathodic regression equation of $y = (2.21x10^{-4} \pm 6.56x10^{-6})x + (6.12x10^{-6} \pm 2.51x10^{-6})$ with $R^2 = 0.9965$.

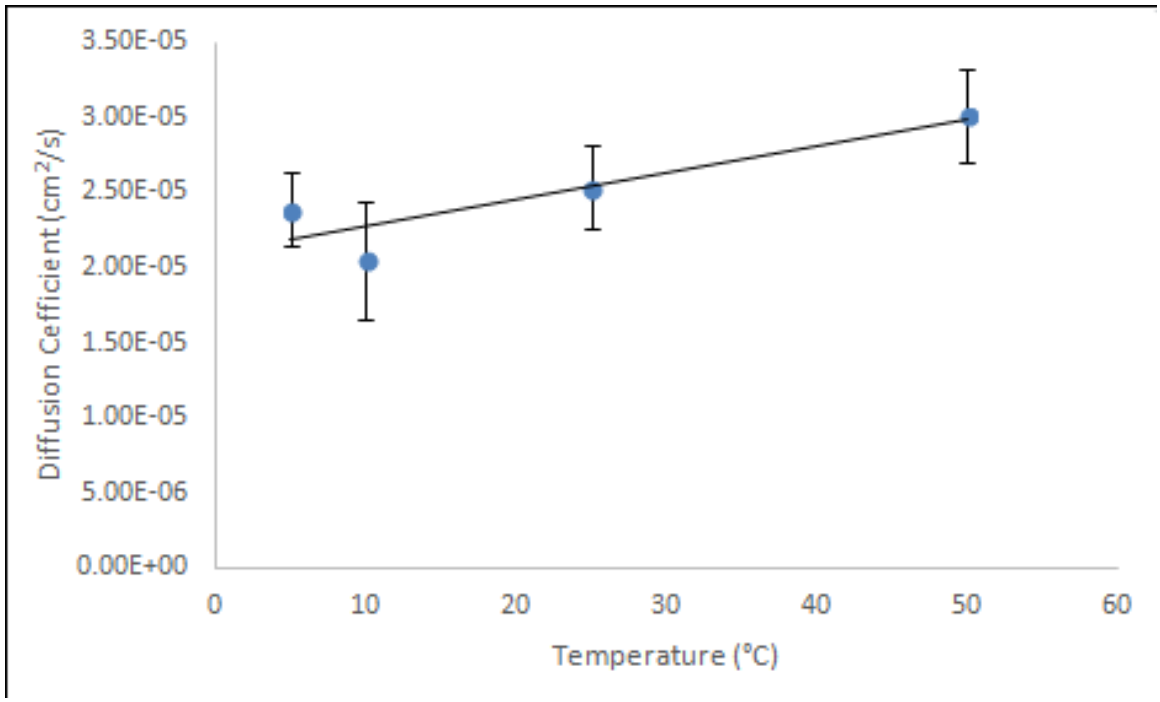

Figure 17. Diffusion coefficients of ferrocene vs. temperature. Regression equation of $y = (1.77x10^{=7} \pm 6.19x10^{-8})x + (2.10x10^{-5} \pm 1.76x10^{-6})$ with $R^2 = 0.8043$..

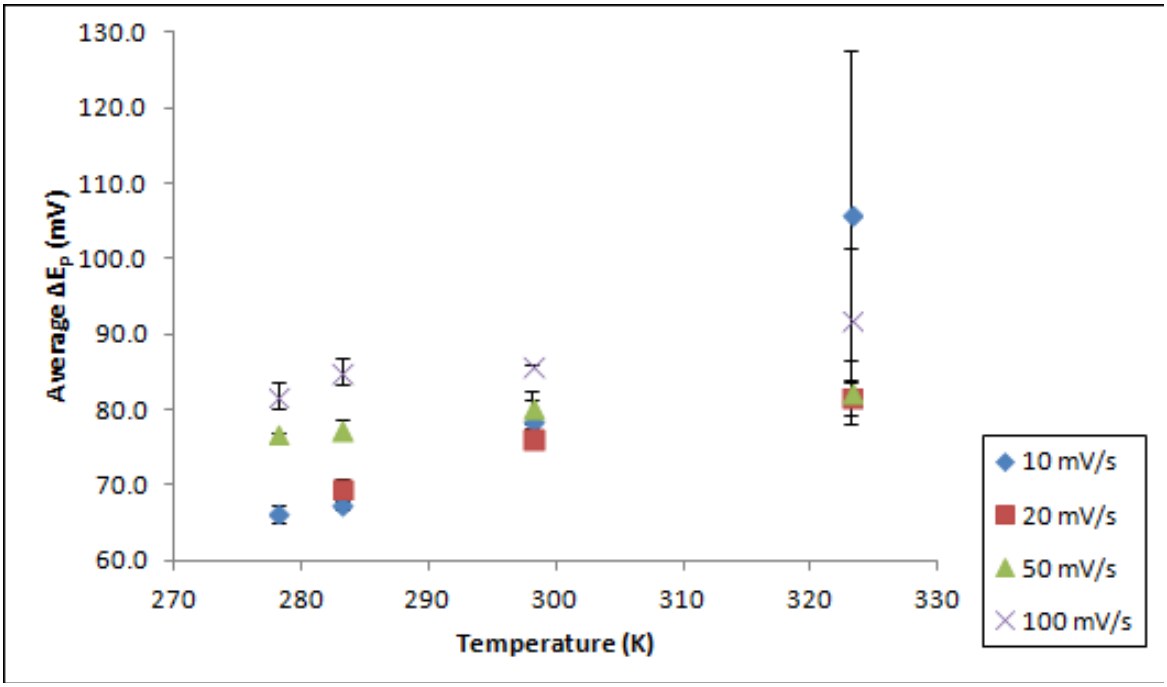

Figure 18. Ferrocene peak splitting as a function of temperature.

most noticeable difference is found with the result from 50 °C There is an abrupt shortening of acetonitrile's solvent window at 50 °C. The observed abrupt change at 50 °C is not understood.

3.2.5 Rate Constants

Based on the peak splitting, standard rate constants k^0 were determined for ferrocene as a function of temperature and temperature. Averaged for all temperatures, the criteria for reversibility is $k^0 \gtrsim (0.46_5 \pm 0.02_6)\, v^{1/2}$. All data for ferrocene are in the reversible electron transfer domain, with k^0 values that are greater than 1 cm/s. The data are not corrected for resistive drop.

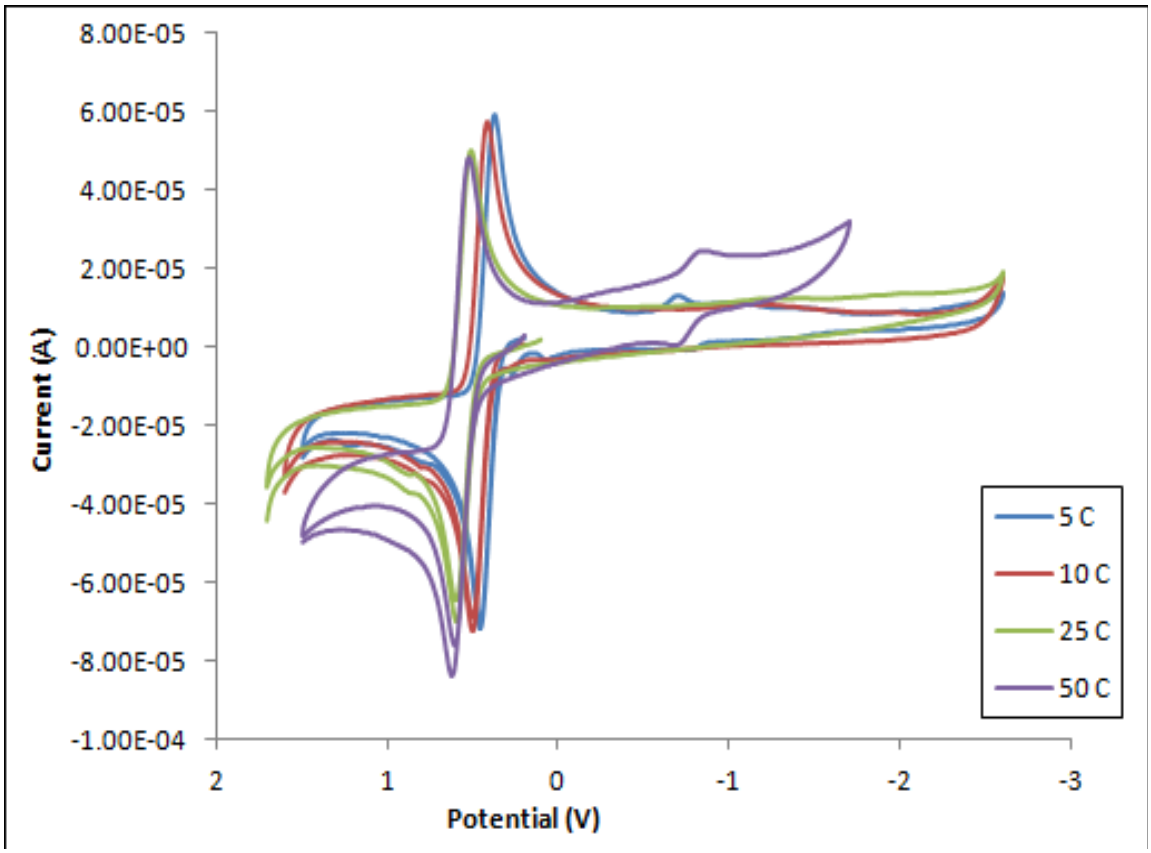

Figure 19. Overlay of cyclic voltammograms of ferrocene at varying temperatures.

CHAPTER 4

CONCLUSIONS

The effect of temperature on the solvent window was examined in nitric acid and in acetonitrile. It was determined that aqueous solutions are more susceptible to expansion of the solvent window at lower temperatures. The aqueous potential window changed from 2.317 V at 70 °C to 2.718 V at 5 °C when examined with a scan rate of 100 mV/s. In addition to the effect of temperature on the available potential range, the temperature influenced the diffusion coefficients of the analytes, the rate constants of the analytes, the standard rate constants of the water oxidation and reduction reactions, and the peak splitting of the analyte.

The analytes' diffusion coefficients increased with increased temperature for both the aqueous and nonaqueous solutions. $[Ru(bpy)_3]^{2+}$'s diffusion coefficients went from 2.63 x 10^{-6}cm^2/s at 5 °C to 9.23 x 10^{-6}cm^2/s at 70 °C. Ferrocene's diffusion coefficients did not increase to the same extent. The diffusion coefficients increased from 2.39 x 10^{-5}cm^2/s at 5 °C to 3.01 x 10^{-5}cm^2/s at 70 °C. The peak splitting also increased with increased temperature, and the results in aqueous and nonaqueous solutions were comparable. At a scan rate of 100 mV/s, $[Ru(bpy)_3]^{2+}$'s peak splitting increased from 67.5 mV at 5 °C to 77.4 mV at 70 °C, while ferrocene's peak splitting went from 82.0 mV at 5 °C to 92.0 mV at 70 °C.

It was also seen that rate constants decreased with decreased temperature for $[Ru(bpy)_3]^{2+}$ and ferrocene. Overall, there was a greater temperature effect on the aqueous solution. It is expected that the lowered standard rate constants of

the water oxidation and reduction reactions contributed to the expanded aqueous solvent window.

CHAPTER 5

FUTURE WORK

First, acetonitrile should be further studied to see if they same behavior that was seen here is reproducible. To determine if the abrupt solvent limit on the reduction wave is due to acetonitrile or to the electrolyte, tetrabutylammonium tetrafluoroborate, the experiments should be repeated with a different electrolyte.

A limited temperature range was examined in this work. For future experiments, lower temperatures approaching the freezing point should be explored to see if the potential window can be extended even more, and to discover if there is a limit to the usefulness of lowering the temperature. Also, examining a larger variety of solvents, aqueous and nonaqueous, would help to understand the effects and differences in the responses to the applied temperatures.

In this study, only reversible redox species were investigated. Examining quasi- and irreversible redox species should also be considered.

REFERENCES

1. Bard, A.J.; Faulkner, L.R. *Electrochemical Methods: Fundamentals and Applications*; John Wiley & Sons, Inc.: New York, 2001.

2. Fry, A.J.; Britton, W.E. *Solvents and Supporting Electrolytes* in *Laboratory Techniques in Electroanalytical Chemistry*. Kissinger, P.T.; Heineman, W.R., Eds.; Marcel Dekker, Inc.: New York, 1984; pp. 367-380.

3. Creager, S. *Solvents and Supporting Electrolytes* in *Handbook of Electrochemistry*. Zoski, C.G., Ed.; Elsevier: Amsterdam, 2007; pp. 51-64.

4. Van Duyne, R.P.; Reilley, C.N. *Low-Temperature Electrochemistry- Characteristics of Electrode Reactions in the Absence of Coupled Chemical Kinetics*. Anal. Chem. **1972**, *44*, 153–158.

5. Tsierkezos, N.G. *Cyclic Voltammetric Studies of Ferrocene in Nonaqueous Solvents in the Temperature Range from 248.15 to 298.15 K*. J. Solution Chem. **2007**, *36*, 289-302.

6. Nicholson, R.S.; Shain, I. *Theory of Stationary Electrode Polarography*. Anal. Chem. **1964**, *36*(4), 706-723.

7. Nicholson, R.S. *Theory and Application of Cyclic Voltammetry for Measurement of Electrode Reaction Kinetics*. Anal. Chem. **1965**, *37*(11), 1351-1355.

8. Paul, H.J.; Leddy, J. *Direct Determination of the Transfer Coefficient from Cyclic Voltammetry: Isopoints as Diagnostics*. Anal. Chem. **1995**, *67*(10), 1661-1668.